

ADVANCED TECHNIQUES OF MAGNETIC RESONANCE IMAGING FOR PROSTATE CANCER

(Essay)

Submitted for partial fulfillment of Master degree in
RADIODIAGNOSIS

by

Mahmoud Mohieldin Mohamed Hassouba

M.B., B.Ch

Supervised by:

PROF. DR. Maha Mohamad Abd Elraoof

Professor of Radiodiagnosis
Faculty of Medicine
Ain Shams University

DR. Rania Mohammed Refaat Abd ElHamid

Lecturer of Radiodiagnosis
Faculty of Medicine
Ain Shams University

**Faculty of Medicine
Ain Shams University**

2015

ACKNOWLEDGMENTS

First and foremost, I thank ALLAH who gave me the strength to accomplish this work.

I wish to express my great indebtedness and deep gratitude to ***Prof. Dr. Maha Mohamed Abd Elraoof***, Professor of Radiodiagnosis, Faculty of Medicine, Ainshams university for accepting the idea of this work, her kind assistance and efforts, which helped me in accomplishing this thesis.

I also extend my thanks and appreciation to ***Dr. Rania Mohammed Refaat Abdelhamid***, Professor of Radidiagnosis, Ainshams university for her valuable guidance and great help in supervising this work. No words can express my feelings, respect and gratitude to her as regards her continuous encouragement and constructive criticism given to me at every stage of this work.

To my parents, brother, sister, cousins and friends especially Dr. Mohamed Ammar, Dr Fatemah Aboelmakarem and Dr Shaimaa Galal, to whom I am overwhelmingly indebted to, thank you and GOD bless you.

I am also deeply grateful to my best friend Dr Mohammed Alsheikh who was always there for me.

CONTENTS

	Page
○ <i>Introduction & Aim of The work</i>	1-3
○ <i>Anatomy of the prostate</i>	4-19
○ <i>Normal MRI Anatomy of the Prostate</i>	20-26
○ <i>Pathology of prostate cancer</i>	27-44
○ <i>Advanced MR techniques used in prostatic imaging</i>	45-67
○ <i>Role of advanced techniques of MRI for prostate cancer with illustrative cases</i>	68-118
○ <i>Summary & Conclusion</i>	119-121
○ <i>References</i>	122-140
○ <i>Arabic Summary</i>	i-ii

LIST OF ABBREVIATIONS

Abbreviation	Name
1.5T	1.5 Tesla
3D	Three-dimensional
3D 1H MRSI	Three dimensional hydrogen proton magnetic resonance spectroscopy imaging
3T	3 Tesla
AAH	Atypical Adenomatous Hyperplasia
ADC	Apparent diffusion coefficient
AFMS	Anterior fibromuscular stroma
AUC	Area under curve
BASING	Band-selective inversion with gradient dephasing
BPH	Benign prostatic hyperplasia
CG	Central gland
Cho	Choline
Cho + Cr / Cit	Choline and creatine to citrate
Cit	Citrate
Cr	Creatine
CT	Computed tomography
CZ	Central zone
DCE	Dynamic contrast enhanced
DHT	Dihydrotestosterone
DRE	Digital rectal examination
DW MRI	Diffusion weighted magnetic resonance imaging

DWI	Diffusion weighted imaging
ECE	Extra capsular extension
ERC	Endorectal coil
FSE	Fast spin echo
Hz	Hertz
IV	Intra venous
kPa	Kilo pascal
Lt	Left
mm	Millimeter
mmol	Millimol
MR	Magnetic resonance
MRI	Magnetic resonance imaging
MRS	Magnetic resonance spectroscopy
MRSI	Magnetic resonance spectroscopy imaging
NVB	Neurovascular bundle
PC	Prostate cancer
PIN	Prostatic intraepithelial neoplasia
ppm	Peak per minute
PRESS	Point-resolved spectroscopy
PSA	Prostatic specific antigen
PZ	Peripheral zone
ROI	Region of interest
Rt	Right

s or sec	Second
SNR	Signal to noise ratio
SV	Seminal vesicles
SVI	Seminal vesicle invasion
T1 WI	T1 weight image
T2 WI	T2 weight image
tCho	Total choline
TNM	Tumor, Nodes, Metastasis
TRUS	Trans rectal ultrasound
TTP	Time to peak
TURP	Transurethral radical prostatectomy
TZ	Transition zone
US	Ultrasonography

LIST OF FIGURES

Figure	Chapter 1 "Anatomy of the prostate "	Page
1	Normal prostate in vertical section with true capsule surrounding	4
2	Graphic Illustrates the relationships between prostate and the male pelvic organs in sagittal view	6
3	Posterior view of prostate and seminal vesicles	7
4	Two graphics illustrate sagittal and corresponding coronal view of male pelvic region	8
5	Graphic illustrates the topography of the posterior wall of the prostatic urethra	9
6	Lobar anatomy of the prostate	11
7	Zonal anatomy of the prostate	12
8	Diagram for prostate in sagittal plane and corresponding axial sections	15
9	Zonal anatomy in sagittal and coronal planes	17
10	Arterial Supply of the Prostate	15
11	Venous Drainage of the Prostate	18
12	Coronal T1MR image of normal young adult prostate	21
13	Axial T1 MR images of the prostate gland.	21
14	Axial T1 MR images of the prostate gland slightly inferiorly.	22
15	Normal zonal anatomy in Axial and Coronal	23
16	Axial T2WI at different levels and Sagittal T2WI shows division of the prostate into three sections in the craniocaudal direction	24
17	Normal prostate zonal anatomy with T2-weighted axial, coronal and sagittal MR images obtained at the level of the seminal vesicles	25
18	Shows T2 weighted axial image of the normal prostate showing NVB	26
Chapter 2 "Pathology of prostate cancer"		
19	The Gleason grading system	25
20	TNM Staging: The four stages of local PC growth	42

Chapter 3 "Advanced MR techniques in prostatic imaging"		
21	MR images and drawings show division of prostate into sextants	49
22	Normal prostate DWI with ADC map	54
23	Illustration for a tissue time signal intensity curve.	58
24	Normal prostate gland depicted with T2-weighted axial MR image and spectra obtained with 1H MR spectroscopy	63
25	MRS metabolic differences between normal zonal anatomy T2W axial image was obtained through the midsection of the prostate	64
26	Axial T2-weighted images with corresponding elastograms spanning the entire prostate from apex to base.	67
Chapter 4 "Role of advanced techniques of MRI for prostate cancer"		
27	Axial, Sagittal and Coronal T2W images of PC in PZ (midgland and apex)	69
28	Axial T1WI of prostatic hemorrhage	69
29	Four different PC cases with ECE viewed in Axial T2WI	71
30	Axial and Coronal T2W images of PC in PZ (midgland and apex)	71
31	T2-weighted axial and coronal MR images in the base of the right lobe with ECE and SVI bilaterally	72
32	Post-operative assessment: Pre-radiation and post-radiation T2WI of three different cases with PC as well as post-salvage radical prostatectomy pathology section	73
33	Local recurrence after radical prostatectomy	74
34	Recurrence after radiation treatment	74
35	Post-operative T2WI, a study that changed patient treatment plan	75
36	T2WI and ADC map images of PC in TZ	77
37	DWI and ADC images of PC in PZ	78
38	DWI and ADC of BPH in CZ	80
39	Residual PC after hormone therapy: ADC with pre and post-operative T2WI	81
40	T2WI and DCE colored images showing PC in PZ	85
41	Fused color map with T2WI for TZ PC	87

42	T2WI and DCE MRI based color coded image in correlation with whole mount histopathologic specimen	88
43	Axial T2WI, unenhanced and post contrast T1WI, color mapped DCE and kinetic curves of PC	89
44	Axial T2WI and pre- and post-contrast T1WI	92
45	Axial T2WI and color mapped DCE showing PC	93
46	Recurrence following prostatectomy, T2WI and DCE curve of scarring and recurrence.	94
47	Recurrence following prostatectomy, T2WI and DCE curve of scarring and recurrence.	95
48	Spectroscopy curve illustrating normal vs PC	98
49	Axial and coronal T2WI and overlaid MRSI curve showing PC in the PZ	99
50	Axial T2WI, Axial ADC map and corresponding MRSI curve of PC with pathology section correlation	100
51	T2WI and MRSI in a patient with suspected local recurrence after radical prostatectomy	101
52	T2WI, DWI and Elastogram showing PC in PZ and TZ	102
53	PIRADS DCE scoring curves	113
54	T2W, DWI, ADC and DCE showing PC in PZ	116
55	T2W, DWI, ADC and DCE showing PC in TZ	118

LIST OF TABLES

Chapter 2 "Pathology of prostate cancer"		
1	Pathological classification of prostate cancer	33
2	Gleason grading scale	37
3	Gleason score	37
4	TNM staging of prostatic cancer	39
Chapter 4 "Role of advanced techniques of MRI"		
5	Parameters of different sequences	96
6	PIRADS for T2WI for PZ	109
7	PIRADS for T2WI for TZ	110
8	PIRADS scoring system for DWI	111

Introduction

Prostate cancer is the most frequently diagnosed cancer in males and the second leading cause of cancer-related death in men (*Bonekamp et al., 2011*).

Detection and localization of prostate cancer is an important given in the emergence of disease- targeted therapies. Knowledge of the tumor location within the prostate can help to direct maximal therapy to the largest focus of tumor while minimizing damage to the surrounding structures, such as the neurovascular bundles, the rectal wall, and the neck of the bladder (*Haider et al., 2007*). Magnetic resonance imaging (MRI) has shown great promise as a noninvasive diagnostic tool in the evaluation and management of prostate cancer (*Mazaheri et al., 2008*).

Recent advances including additional functional and physiologic MRI techniques allow extension of the obtainable information beyond anatomic assessment (*Bonekamp et al., 2011*).

Multi parametric magnetic resonance imaging includes diffusion-weighted imaging (DWI), dynamic contrast enhanced MRI (DCE MRI) and magnetic resonance spectroscopy (MRS). These new MRI techniques are increasingly being used to supplement conventional T2 and T1-weighted MR sequences in prostate imaging (*Franiel, 2011*).

MR spectroscopy is a promising development in the radiological evaluation of possible prostate malignancy (*Westphalen et al., 2008*).

MR Elastography is a new imaging method with potential in the diagnosis of prostate cancer (*Li et al., 2011*).

Furthermore, MRI has been used for follow-up of prostate cancer after irradiation therapy, hormonal ablation, and cryosurgery (*Graser et al., 2007*).

Aim of the work

To highlight the role of the advanced MRI techniques in accurate detection, localization, staging and post treatment follow up of prostate cancer.

Anatomy of the prostate

The prostate is the largest accessory gland of the male reproductive system (*Keith and Agur, 2007*), normally it is a conically shaped organ about the size of a walnut and is situated deep in the male pelvis (*Barker et al., 2010*). The gland is 4 cm transversely, 2 cm in anteroposterior and 3 cm in its vertical diameters, and weighs 8 g in youth, but invariably enlarges with the development of benign prostatic hyperplasia (BPH) (*Standring, 2008*).

The prostate is a fibromuscular gland which surrounds the prostatic urethra from the bladder base to the membranous urethra and is itself surrounded by a thin but tough connective tissue capsule. Being somewhat pyramidal, it presents a base or vesical aspect superiorly, an apex inferiorly and posterior, anterior and two inferolateral surfaces (**Fig1**) (*Standring, 2008*).

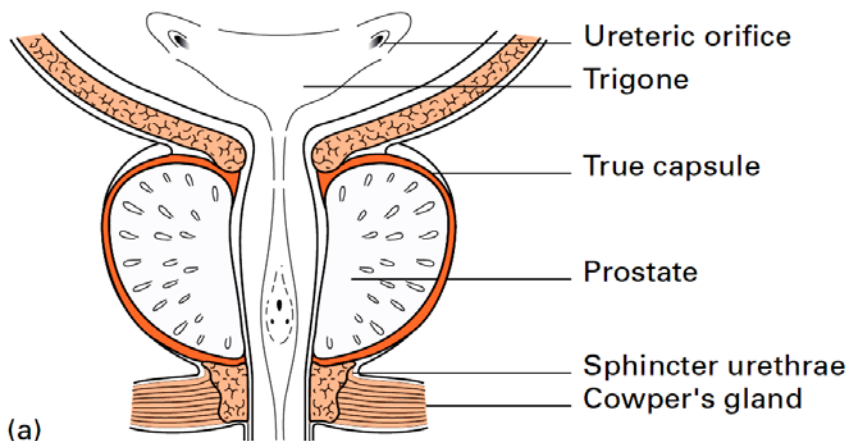


Fig (1): Normal prostate in vertical section with true capsule surrounding
(Quoted from *Ellis, 2006*).

Superiorly its base is largely continuous with the neck of the bladder. The urethra enters it near its anterior border (**Fig2**) (*Ellis, 2006*).

The apex is inferior, surrounding the junction of the prostatic and membranous parts of the posterior urethra (*Standring, 2008*). It is in contact with fascia on the superior aspect of the urethral sphincter and deep perineal muscles (*Keith and Agur, 2007*),

The anterior surface lies in the arch of the pubis, separated from it by a venous plexus (Santorini's plexus) and loose adipose tissue (extraperitoneal fat) in the retropubic space (cave of Retzius). It is extending from the apex to the base and near its superior limit it is connected to the pubic bones by the puboprostatic ligaments. The urethra emerges from this surface anterosuperior to the apex of the gland, it is relatively deficient in glandular tissue and is largely composed of fibromuscular tissue (**Fig2**) (*Standring, 2008*).

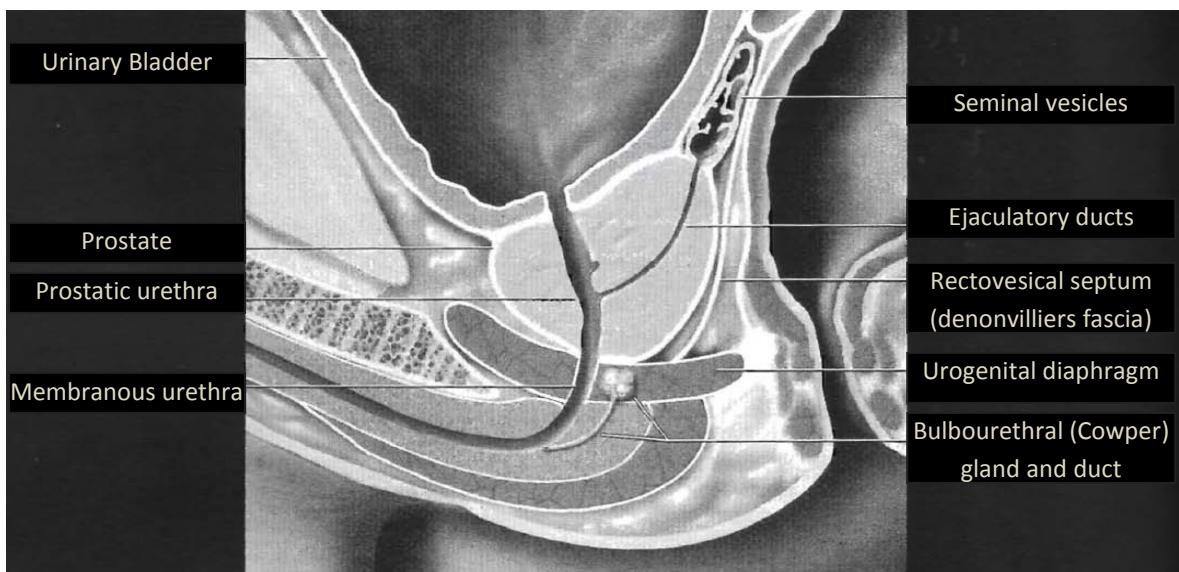


Fig (2): Graphic illustrates the relationships of prostate gland with the male pelvic organs. The prostate surrounds the upper part of urethra. The base of the prostate is in direct contact with the neck of the urinary bladder and its apex is in contact with the superior fascia of urogenital diaphragm. The posterior surface is separated from rectum by rectovesical septum (Denonvilliers fascia) (*Quoted from Federle et al., 2006*).

The posterior surface is separated from the rectum by Denonvillier's fascia, a dense condensation of pelvic fascia which develops by obliteration of the rectovesical peritoneal pouch (**Fig2**). The posterior surface is transversely flat and vertically convex. Near its superior (juxtavesical) border is a depression where it is penetrated by the two ejaculatory ducts (**Fig3**). Below this is a shallow, median sulcus, usually considered to mark a partial separation into right and left lateral lobes (*Standring, 2008*).